Universal dynamics of coarsening during polymer-polymer thin-film spinodal dewetting kinetics

J. Lal,[1,2,3] L. B. Lurio,[3] D. Liang,[2] S. Narayanan,[4] S. B. Darling,[5] and M. Sutton[6]
[1]*Materials Science Division, Argonne National Laboratory, Argonne, Illinois 60439, USA*
[2]*Intense Pulsed Neutron Source, Argonne National Laboratory, Argonne, Illinois 60439, USA*
[3]*Department of Physics, Northern Illinois University, DeKalb, Illinois 60115, USA*
[4]*X-ray Science Division, Argonne National Laboratory, Argonne, Illinois 60439, USA*
[5]*Chemical Sciences and Engineering, Argonne National Laboratory, Argonne, Illinois 60439, USA*
[6]*Physics Department, McGill University, Montréal, H3A 2T8, Canada*

(Received 22 April 2020; revised 30 June 2020; accepted 23 August 2020; published 10 September 2020)

The dewetting dynamics of a supported bilayer polymer thin film on a solid substrate is investigated using grazing incidence x-ray photon correlation spectroscopy. We find that the top layer dewets via the spinodal mechanism. The kinetics of the dewetting is studied by monitoring the time evolution of the surface diffuse x-ray scattering intensity. We study the time evolution of fluctuations about the average surface structure by measuring the two-time x-ray intensity fluctuation correlation functions. Using these two-time correlation functions we quantify the crossover from early-time diffusive dynamics to hydrodynamics. The early diffusive regime satisfies dynamic universality. The two-time correlation functions also quantify the onset of hydrodynamic effects. The hydrodynamic regime is observed during the spinodal dewetting process as these interactions are not screened.

DOI: 10.1103/PhysRevE.102.032802

I. INTRODUCTION

Fluctuations in nonequilibrium states grow or decay on mesoscopic scales in a self-similar manner [1]. We present an experimental study of fluctuations in the x-ray scattering intensity from a nonequilibrium dewetting system undergoing coarsening by domain growth, where the patterns at different times are statistically similar. Dewetting is segregation of like molecules which come together on the surface. There is a close analogy between dewetting and bulk phase separation, where the film height fluctuations plays the role of the composition fluctuations in the bulk case [2]. Dynamical scaling and dynamical universality have given a unified, time-independent description of the statistical structure of phase-separating materials in the diffusive coarsening regime [3–5]. Here we examine how and to what extent spinodal dewetting in viscoelastic polymer thin films on a soft substrate is analogous to spinodal decomposition in bulk phase-separating materials. X-ray scattering can measure the time evolution of average surface structural correlations in a material undergoing spinodal dewetting. In addition, coherent x-ray speckle can be used to probe fluctuations about this evolving average surface structure, through x-ray photon correlation spectroscopy (XPCS), which are otherwise invisible [6].

The original model [7] for studying the rupture of soap films was developed [8] for investigating thin liquid films spinodally dewetting due to amplification of capillary wave fluctuations on solid substrates. This was further generalized to spinodal dewetting on liquid substrates [9]. The dewetting of a molten polymer thin film on a molten polymer melt substrate is a more complicated than the more commonly studied polymer-solid case [2,10,11], because the polymer-polymer interface exhibits slip boundary condition, and thus both the buried interface and the free film surface are deformable [12–16].

The evolution of polymer-polymer dewetting, as with the bulk phase separation process, can be divided into a number of different regimes [17]. In the early stage, fluctuations are amplified, due to the unstable free energy, and grow exponentially, with the dynamics dominated by the fastest growing mode. Once phase separation has occurred, the system enters the coarsening stage. In early stage coarsening, driven by concentration or thickness gradients, one length scale, L, is necessary to describe coarsening, and the time dependence of this length scale has a power law, $L \sim t^n$ with growth exponent $n = 1/3$ for conserved order parameter. This is expected to be same in $d = 2$ and $d = 3$ dimensions [4,18] as these exponents are super-universal. The growth exponents depend on only a few properties of the underlying system, i.e., even fewer properties than the critical exponents. In the very late stages, this scaling fails in fluid systems due to dynamics being dominated by hydrodynamic flows instead of diffusion [19].

Thicker polymer films dewet by nucleation process [20–25] whereas thinner films via the spinodal mechanism [2,10,11,13] on both solid and liquid substrates [9], as shown by AFM measurements. The early stages of polymer-polymer spinodal dewetting [Fig. 1(a)] were characterized *in situ* for the first time by grazing incidence neutron scattering, but the detailed kinetics of the process were not explored due to sparsity of data [12]. In the present work we are in the later stages of spinodal dewetting in the coarsening regime on a liquid substrate not explored in the literature [Fig. 1(c)].

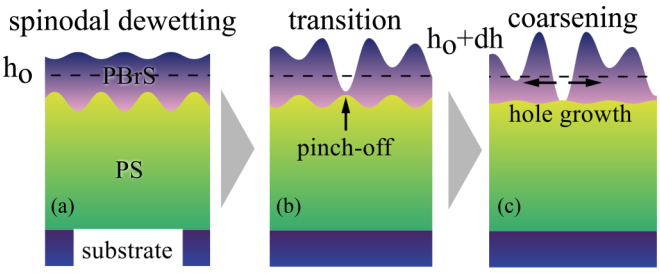

FIG. 1. Schematic snapshots of the time evolution of a two-layer PBrS-PS film on a Si substrate with slip at the PBrS-PS interface. (a) Idealized schematic of the "peristaltic mode" leading to dewetting, where the displacements of the free surface and the polymer-polymer interface are in antiphase [9]. (b) At the film rupture point the hole depth becomes comparable to the top film thickness h. This is confirmed by AFM measurements, where the average depth of the holes is equal on average to the top-layer thickness. (c) The late-stage coarsening of the film that is followed *in situ* by the XPCS experiments reported in the present work.

We show below that the diffusive regime is followed by hydrodynamic regime like in bulk phase separation in binary fluids [17,19]. For slip boundary conditions, growth laws in the hydrodynamic regime are observed during dewetting [26], while for stick boundary conditions hydrodynamic interactions are to a large extent screened, and only the diffusive regime ($n = 1/3$) is observed for a polymer thin film on a solid substrate [2]. We report below nonequilibrium scaling of the correlation time from the two-time correlation function made possible by the use of coherent x-rays in the diffusive regime which could not be accessed in earlier work [2], which reports just the Fourier transform of the AFM spectra. Further, in analogy to bulk phase separation, these late-stage coarsening regimes would be the same whether the holes formed initially by spinodal or nucleation mechanism [17].

We quantify the dewetting process through two distinct measures. First, the self-similar evolution of the average dewetting structure is measured through the time evolution of the average diffuse scattering, $I(q_\parallel, t)$. Second, we quantify the time evolution of fluctuations about the average via measurement of the two-time correlation function (TTCF), $C(q_\parallel, t_1, t_2)$ which can be obtained by time correlation of the speckle pattern resulting when the sample is illuminated using a coherent incident x-ray beam [6].

II. METHODS

The system studied here is a poly(4-bromo styrene) (PBrS) thin film deposited on an immiscible and nonwettable polystyrene (PS) sublayer on a silicon substrate. Monodisperse PS samples (molecular weights $M_w = 1500$ kDa) from Pressure Chemical were used. The thickness of the PS bottom layer was fixed to 1000 Å and was deposited on precleaned 15×15 mm silicon wafers. The PBrS ($M_w = 350$ kDa, the fraction of brominated monomers was 0.89) was used as the top layer. The bilayers were prepared by spin coating from toluene solution PBrS layers of thickness ~200 Å onto a glass slide. This thin layer was then floated from deionized water onto the 1000 Å PS sublayer on the silicon substrate. The bilayer film was annealed at 90 °C (so not to initiate dewetting) for 12 h. This temperature is below the glass transition temperature of PS ($T_g = 100$ °C) and PBrS (100% brominated PBrS, $T_g = 142$ °C [25,27,28]). There was additional annealing of the PBrS layer (reptation time 43 s) prior to observation window of the kinetics (the $t_w = 512$ s after quench at 155 °C). There is a strong slip boundary condition which causes less stress at the buried interface, thus, the bulk of the dewetting dynamics will represent the properties of the equilibrated sample [28].

Grazing-incidence XPCS experiments were performed at the x-ray energy of 7.35 keV with beam size 20 μm×20 μm at the sector 8-ID-I beamline at the Advanced Photon Source, Argonne National Laboratory, as described previously [14]. The kinetics of dewetting was followed *in situ* via diffuse surface x-ray scattering, recorded by successive detector frames. The exposure time was 0.05 s per frame, and the time interval between frames was 1.99 s. Partially coherent x-rays are incident at 0.198°, which is below the critical angle for total external reflection. In order to perform x-ray scattering measurements, the samples were placed in a temperature-controlled vacuum chamber (~10^{-4} torr). Dewetting of PBrS thin films is followed above T_g of both layers *in situ* using XPCS.

The PBrS/PS bilayers are unstable, and, if heated above the glass transition, the top surface dewets from the PS-coated substrate. Experimentally, it was found that these strongly immiscible films have a thin interface (~25 Å) where polymers intermix mostly on the segmental scale. The interdiffusion is small [15,16]. The effect of the fluidity of the bottom layer is to create a slip boundary condition for the top layer [16] since the slip length at the interface exceeds the 200 Å thickness of the top layer [28]. The bulk dynamics of the bottom layer do not play a significant role due to the high viscosity of the PS, which acts like an almost solid substrate [9,12,28,29].

III. RESULTS AND DISCUSSION

Dewetting begins via capillary wave fluctuations at the top interface [7,30] [Fig. 1(a)]. Once the capillary wave amplitude becomes comparable to the top film thickness, rupturing or pinch-off [19,31,32] starts along the troughs [Fig. 1(b)]. Once holes open, further dewetting of the top film proceeds via prolonged coarsening of the still connected structure. This late-time regime [Fig. 1(c)] is the focus of the present paper.

For polymer thin-film systems, the dewetting can be described successfully by the effective interface potential $\phi(h)$ (h is thickness of the top film), which is a sum of short- and long-range interactions [33]. The latter are dominated by van der Waals interactions. Their strength can be obtained by calculating the Hamaker constant via the optical properties of the involved media [34]. Following previous work [13,33], the total surface potential of the bilayer film and its derivative is calculated as the function of the thickness of the top layer. For the thickness of the top PBrS layer here, $\phi''(h_o) < 0$ which confirms that the top layer dewets spinodally. We have also calculated the dominant rupture length scale λ_c for dewetting via the spinodal mechanism using the calculated value of

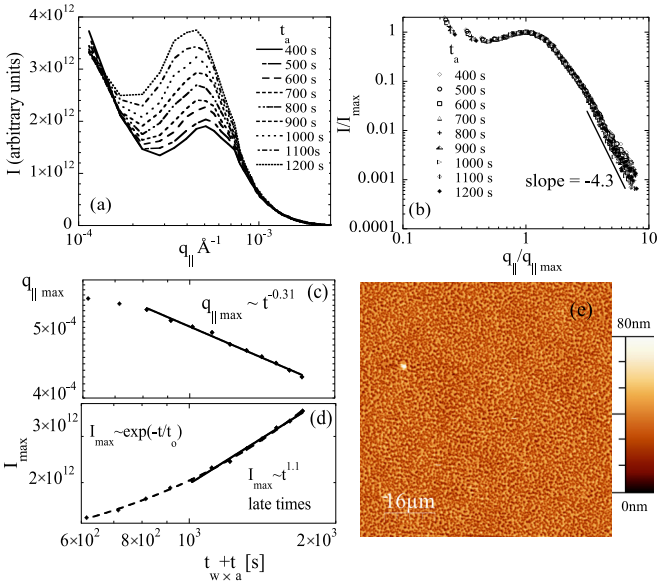

FIG. 2. (a) Time evolution of the one-time diffuse scattering structure factor at different times. The data are shown for $t_w = 512$ s after quench. (b) Scaling behavior of the average diffuse scattering structure factor $I/I_{\max}$ versus $q_\parallel/q_{\parallel\max}$ at different times after the start of the dewetting. (c) Wave vector $q_{\parallel\max}$ versus time after quench. (d) Intensity $I_{\max}$ versus time after quench, $t_o = 1149.4$ s in the exponential fit. (e) AFM topography showing the dewetting pattern for the bilayer. This was taken after the XPCS measurements (121 minutes in the x-ray beam at 155 °C).

$\phi''(h_o)$ [13]. This calculation is shown in detail [28]. The characteristic length scales observed in the experimental data are of the same order of magnitude as the critical λ_c calculated from $\phi''(h_o)$ [28].

We first present results similar to critical quenches in binary fluids (equal volume fractions of the two species) [35]. We are in the late stages of growth when domain boundaries are already well developed [28]. As time goes on, the domains grow so as to minimize the area of the domain walls that separate the dewetted holes from the connected film [Figs. 2(a)–2(e)]. The data in Figs. 2(a) and 2(b) are shown for $t_w = 512$ s after quench. Estimates of intensity $\langle I\rangle_{\max}(t)$ and the in-plane scattering wave vector $q_{\parallel\max}(t)$ were obtained by fitting the near-peak regions of $\langle I\rangle(q_\parallel)$ at each time step with a Gaussian after having taken into consideration the background intensity using a polynomial [Fig. 2(a)]. Figure 2(a) shows the diffuse in-plane scattering intensity as a function of $q_\parallel$. With increasing time from the quench the amplitude of the structural peak increases and moves to smaller $q_\parallel$ as expected for spinodal dewetting. A stronger test of scaling is given by whether the scattering function itself scales. The data in Fig. 2(a) can be scaled by rescaling the $q_\parallel$ axis as $q_\parallel/q_{\parallel\max}$ and the amplitude as $I/I_{\max}$, where $I_{\max}$ is the amplitude of the peak intensity. Figure 2(b) shows this scaling, where all intensity curves fall onto a universal line similar to the spinodal decomposition in bulk systems (small deviations at large and low $q_\parallel$). Initially, the diffusive transport is driven by height (like composition) gradients. The very early data points slow growth of $q_{\parallel\max}$ followed by $q_{\parallel\max} \sim t^{-0.31}$ which is consistent with Ref. [2] and is also as typically observed [3,4,35] in other phase-separating materials in bulk [Fig. 2(c)]. While $I_{\max}$ can be fitted to an exponential, it becomes more linear over time [Fig. 2(d)]. An additional consistency check on the analysis of the experimental data is the expected relation $\beta = 3\alpha$, where α and β are, respectively, the time exponents defined by $q_{\parallel\max} \sim t^{-\alpha}$ and $I_{\max} \sim t^{\beta}$. $I_{\max}$ grows almost linear at late times consistent with $q_{\parallel\max} \sim t^{-0.31}$ [28]. The coarsening seen above corresponds to the diffusive coarsening regime during phase separation in systems such as binary alloys [4], fluid mixtures [35], and sodium borosilicate glass [3] in which the scalar order parameter is conserved.

The atomic force microscopy (AFM) image of the surface topography of the bilayer at the end of the x-ray measurements (after 121 minutes) is shown in Fig. 2(e). Holes of uniform size and uniformly distributed in the still connected top layer are observed. This AFM scan seem of similar form (the holes here are more disconnected due to longer annealing and coarsening in diffusive and hydrodynamic regime) to the SFM topography data of early spinodal dewetting data [13].

The time evolution of a 400-pixel-wide single row of a speckle pattern are shown in [28], taken from surface diffuse scattering during dewetting, which we denote a "waterfall" plot [36]. Time evolution of a single row of pixels in the waterfall plot shows persistent nonequilibrium fluctuations for long periods of time [28,37]. The speckle correlations are analyzed using the TTCF defined via [14]

$$C(q_\parallel, t_1, t_2) = \frac{\langle I(q_\parallel, t_1)\, I(q_\parallel, t_2)\rangle}{\langle I(q_\parallel, t_1)\rangle\, \langle I(q_\parallel, t_2)\rangle}. \tag{1}$$

Here $\langle\cdots\rangle$ denotes averaging over pixels at equivalent wave vectors. The TTCF measures how structure on a given length scale changes between time t_1 and time t_2 as the sample evolves. The TTCF is plotted in Fig. 3(a) for $q_\parallel \sim 3.34\times10^{-4}$ Å^{-1}. We demonstrate below that this TTCF also satisfies dynamic scaling during the spinodal dewetting process as previously observed during the bulk phase separation process [3,4].

Figure 3(a) shows that the correlations $C(q_\parallel, t_1, t_2)$ depend on both time arguments t_1 and t_2. For comparison, in an equilibrium system, these correlations would only depend on $t_1 - t_2$ and all contours would be parallel to the diagonal. For the nonequilibrium system, $C(q_\parallel, t_1, t_2)$ show correlation times that increase with total time [Fig. 3(a)]. The natural variables describing TTCFs are the "dewetting time" $t_a = (t_1 + t_2)/2$, measured along the $t_1 = t_2$ diagonal and the time difference $t = |t_1 - t_2|$ corresponding to the distance from the same diagonal. The "one-time" slices $t_a = \text{const}$ [Fig. 3(b)] are fitted to give a characteristic correlation time τ, which can be taken as the time at which "one-time" slices of $C(q_\parallel, t_1, t_2)$ fall to 0.5 [4]. Based on a moving interface model, an analytical form for this normalized TTCF can be derived [37–39]

$$C(z) = \left[z^2\, \frac{K_2(z)}{2}\right]^2, \tag{2}$$

where $K_2(z)$ is a modified Bessel function of the second kind and the scaling variable is $z = At/t_a^{2/3}$, where A makes z dimensionless [Fig. 3(c)]. This form provides a good fit to

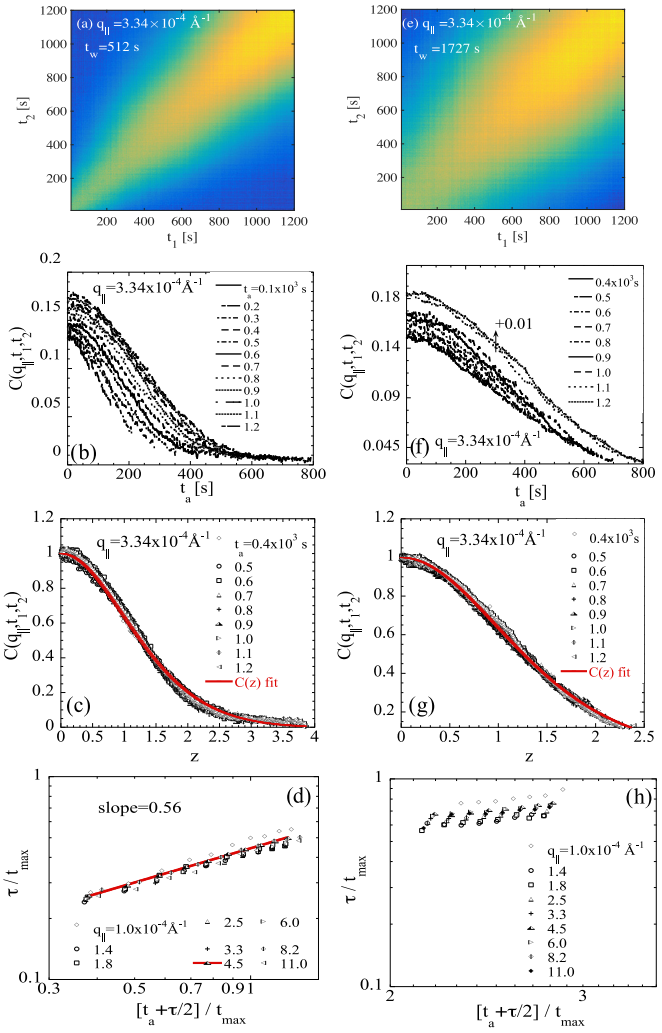

FIG. 3. Fluctuations during domain coarsening. (a) TTCF at $q_\parallel = 3.34\times10^{-4}$ Å^{-1} at 155 °C, $t_w = 512$ s after quench. (b) "One-time" slices t_a = constant, as described in the text. (c) Normalized TTCF with $z = At/t_a^{2/3}$. The red line shows an analytical fit defined by $C(z)$ [Eq. (2)]. (d) Scaled correlation times (obtained from from the one-time slices) for different in-plane wave vectors. The red line is a power-law fit to the data. (e)–(h) Same plots as (a)–(d) at later $t_w = 1727$ s; details in text.

the data. Further, Fig. 3(d) shows the measured correlation times τ versus t_a. In the diffusive regime the dewetting process follows a universal behavior. At large $q_\parallel$ and late times $\tau \sim t_a^{2/3}$ [37,38]. Here τ is the measured decay rate of the correlation function normalized by $t_{\max}$, the time for which the intensity is a maximum at constant $q_\parallel$ [Fig. 3(d)]. This scaling $2/3 = 1 - n$ reflects interface fluctuations of the dewetted holes during the coarsening process and is directly related to Porod's law, in agreement with simulations [37,38].

The initial stage of the phase separation is diffusive; and the hydrodynamic stage of the process follows afterwards in binary fluids [35,40]. This is shown first through the one-time structure scaling, where $\beta = 3\alpha$ holds for the exponents of $q_{\parallel\max}(t)$ and $I_{\max}(t)$ throughout the hydrodynamic regime as shown for later snapshots with increasing time (see Figs. 4–6 in Ref. [28]). The value of α increases up to 0.76 [see Fig. 5(a) in Ref. [28]]. In the viscous hydrodynamic regime the maximum value of α is 1 [41]. The last time snapshot shows a value $\alpha = 0.72$ [see Fig. 6(a) in Ref. [28]]. In the inertial hydrodynamic regime, $\alpha = 2/3$ [42]. These exponents have been discussed extensively in the context of domain coarsening during spinodal decomposition in binary fluid mixtures [19,31,43–45]. These growths laws in this regime could be limited due to viscoelastic effects [46].

Further, after scaling the scattering curves by $q_{\parallel\max}$ and $I_{\max}$, the data at all times fall on the same master curve except at the very large $q_\parallel$ [Fig. 2(b)]. Normally, we observe Porod's law at large $q_\parallel$ due to the presence of sharp well-defined interfaces. The asymptotic behavior $q_\parallel/q_{\parallel\max} > 1$ is greater than the Porod's exponent of 4, due to curvature corrections [47]. This exponent steadily increases with time as shown by our data [28] as the domains become more circular.

Later, the TTCF shows several features which do not agree with the expectations of diffusive dynamics. Figures 3(e)–3(h) show the same plots as Figs. 3(a)–3(d) later in time $t_w = 1727$ s. (For this batch $\alpha = 0.4 \pm 0.02$, $\beta = 1.58 \pm 0.02$ [28], $I_{\max}$ grows slightly faster than the expected $\beta = 3\alpha$). Here we start to observe the onset of hydrodynamic effects on large length scales (at low $q_\parallel$, curves are slightly offset for clarity) [Fig. 3(f)]. These effects were observed in early works on fluid mixtures with increasing values of exponent α greater than 1/3 and non-Lorentzian power spectra [40] also, at the onset of flows around large dewetting holes formed by nucleation [see Fig. 1(g) in [14]]. $C(q_\parallel, t_1, t_2)$ scales in time as $C(z)$ [Fig. 3(g)], but different values of τ do not collapse to a single curve with wave vector [Fig. 3(h)]. $C(q_\parallel, t_1, t_2)$ as a function of $q_\parallel$ are shown for the different snapshots with increasing time [28]. As expected [31,43,48], for large-scale hydrodynamic flows, strong fluctuations in $C(q_\parallel, t_1, t_2)$ at low $q_\parallel$ compared to large $q_\parallel$ are observed. We interpret these deviations as resulting from a transition to the hydrodynamic flow regime.

IV. CONCLUSION

We have measured speckle evolution and its time correlations, which reveal the underlying fluctuation dynamics responsible for the average kinetic evolution of domain coarsening in a thin film undergoing spinodal dewetting (on a soft sublayer). The static structure factor scales with a peak wave vector that varies as $t^{-0.31\pm0.01}$ in the diffusive regime, while the dynamics shows a universal form which scales as the average time, $\tau \sim t_a^{0.56\pm0.01}$. This scaling of the correlation time in the short diffusive regime of coarsening observed during polymer-polymer spinodal dewetting with high viscosities is similar to that seen in the bulk phase separation in borosilicate glass and Al-Li alloy [3,4] where TTCFs $\tau \sim t_a^{2/3}$ ($2/3 = 1 - n$). This establishes the close analogy between the processes of thin-film spinodal dewetting on a polymeric underlayer and bulk phase separation. Although very different, these systems display the same dynamic scaling of fluctuations [37–39] thus demonstrating dynamic universality. We note that we do not reach the late asymptotic diffusive regime (lowest $q_\parallel$ already shows small hydrodynamic

effect), but we show instead further in time the onset of hydrodynamics unique to fluid mixtures. In this regime, the scaling of $C(q_\parallel, t_1, t_2)$ as $C(z)$ with time still applies, but as a function of $q_\parallel$ the scaling of the correlation time extracted from $C(q_\parallel, t_1, t_2)$ does not. These experimental observations may guide the development of improved models for late-stage bulk phase separation in binary fluids [31] as well as interfacial flows during domain coarsening in thin films.

ACKNOWLEDGMENTS

This research used resources of the Advanced Photon Source and the Center for Nanoscale Materials, U.S. Department of Energy (DOE) Office of Science User Facilities operated for the DOE Office of Science by Argonne National Laboratory under Contract No. DE-AC02-06CH11357. We also acknowledge Dr. T. Kawaguchi for his help with the schematic illustration.

[1] H. Furukawa, $1/f$ noise and turbulence from a self-similar decay of fluctuation, Prog. Theor. Phys. **73**, 1141 (1985).

[2] R. Xie, A. Karim, J. F. Douglas, C. C. Han, and R. A. Weiss, Spinodal Dewetting of Thin Polymer Films, Phys. Rev. Lett. **81**, 1251 (1998).

[3] A. Malik, A. R. Sandy, L. B. Lurio, G. B. Stephenson, S. G. J. Mochrie, I. McNulty, and M. Sutton, Coherent X-Ray Study of Fluctuations During Domain Coarsening, Phys. Rev. Lett. **81**, 5832 (1998).

[4] F. Livet, F. Bley, R. Caudron, E. Geissler, D. Abernathy, C. Detlefs, G. Grübel, and M. Sutton, Kinetic evolution of unmixing in an AlLi alloy using x-ray intensity fluctuation spectroscopy, Phys. Rev. E **63**, 036108 (2001).

[5] N. Mason, A. N. Pargellis, and B. Yurke, Scaling Behavior of Two-Time Correlations in a Twisted Nematic Liquid Crystal, Phys. Rev. Lett. **70**, 190 (1993).

[6] M. Sutton, A review of x-ray intensity fluctuation spectroscopy, C. R. Phys. **9**, 657 (2008).

[7] A. Vrij, Possible mechanism for the spontaneous rupture of thin, free liquid films, Discuss. Faraday Soc. **42**, 23 (1966).

[8] F. B. Wyart and J. Daillant, Drying of solids wetted by thin liquid films, Can. J. Phys. **68**, 1084 (1990).

[9] F. Brochard Wyart, P. Martin, and C. Redon, Liquid/liquid dewetting, Langmuir **9**, 3682 (1993).

[10] G. Reiter, Dewetting Of Thin Polymer Films, Phys. Rev. Lett. **68**, 75 (1992).

[11] G. Reiter, Unstable thin polymer films: Rupture and dewetting processes, Langmuir **9**, 1344 (1993).

[12] M. Sferrazza, M. Heppenstall-Butler, R. Cubitt, D. Bucknall, J. Webster, and R. A. L. Jones, Interfacial Instability Driven by Dispersive Forces: The Early Stages of Spinodal Dewetting of a Thin Polymer Film on a Polymer Substrate, Phys. Rev. Lett. **81**, 5173 (1998).

[13] J. P. de Silva, M. Geoghegan, A. M. Higgins, G. Krausch, M.-O. David, and G. Reiter, Switching Layer Stability in a Polymer Bilayer by Thickness Variation, Phys. Rev. Lett. **98**, 267802 (2007).

[14] J. Lal, S. Malkova, M. K. Mukhopadhyay, S. Narayanan, A. Fluerasu, S. B. Darling, L. B. Lurio, and M. Sutton, Dewetting in immiscible polymer bilayer films, Phys. Rev. Materials **1**, 015601 (2017).

[15] X. Hu, X. Jiao, S. Narayanan, Z. Jiang, S. Sinha, L. B. Lurio, and J. Lal, Resonantly enhanced off-specular x-ray scattering from polymer/polymer interfaces, Eur. Phys. J. E **17**, 353 (2005).

[16] X. Hu, Z. Jiang, S. Narayanan, X. Jiao, A. R. Sandy, S. K. Sinha, L. B. Lurio, and J. Lal, Observation of a low-viscosity interface between immiscible polymer layers, Phys. Rev. E **74**, 010602(R) (2006).

[17] R. A. L. Jones, *Soft Condensed Matter*, Oxford Master Series in Physics (Oxford University Press, Oxford, 2002).

[18] L. Sung, A. Karim, J. F. Douglas, and C. C. Han, Dimensional Crossover in the Phase Separation Kinetics of Thin Polymer Blend Films, Phys. Rev. Lett. **76**, 4368 (1996).

[19] V. M. Kendon, J.-C. Desplat, P. Bladon, and M. E. Cates, 3D Spinodal Decomposition in the Inertial Regime, Phys. Rev. Lett. **83**, 576 (1999).

[20] G. Reiter, Dewetting of Highly Elastic Thin Polymer Films, Phys. Rev. Lett. **87**, 186101 (2001).

[21] D. Peschka, S. Bommer, S. Jachalski, R. Seemann, and B. Wagner, Impact of energy dissipation on interface shapes and on rates for dewetting from liquid substrates, Sci. Rep. **8**, 13295 (2018).

[22] P. Lambooy, K. C. Phelan, O. Haugg, and G. Krausch, Dewetting at the Liquid-Liquid Interface, Phys. Rev. Lett. **76**, 1110 (1996).

[23] K. Kostourou, D. Peschka, A. Münch, B. Wagner, S. Herminghaus, and R. Seemann, Interface morphologies in liquid/liquid dewetting, Chem. Eng. Process. **50**, 531 (2011).

[24] R. A. Segalman and P. F. Green, Dynamics of rims and the onset of spinodal dewetting at liquid/liquid interfaces, Macromolecules **32**, 801 (1999).

[25] D. Slep, J. Asselta, M. H. Rafailovich, J. Sokolov, D. A. Winesett, A. P. Smith, H. Ade, and S. Anders, Effect of an interactive surface on the equilibrium contact angles in bilayer polymer films, Langmuir **16**, 2369 (2000).

[26] A. Winkler, P. Virnau, K. Binder, R. G. Winkler, and G. Gompper, Confinement-induced screening of hydrodynamic interactions and spinodal decomposition: Multiscale simulations of colloid-polymer mixtures, Europhys. Lett. **100**, 46003 (2012).

[27] S. Huettenbach, M. Stamm, G. Reiter, and M. Foster, The interface between two strongly incompatible polymers: Interfacial broadening and roughening near T_g, Langmuir **7**, 2438 (1991).

[28] See Supplemental Material at http://link.aps.org/supplemental/10.1103/PhysRevE.102.032802 for detailed calculation of interface potential, its derivative and other parameters of the bilayer, the experimental set up, the waterfall plot and plots of the scaling of one-time correlation functions and q-dependence of two-time correlation functions in the hydrodynamic regime.

[29] A. M. Higgins, M. Sferrazza, R. A. L. Jones, P. C. Jukes, J. S. Sharp, L. E. Dryden, and J. Webster, The timescale of spinodal dewetting at a polymer/polymer interface, Eur. Phys. J. E **8**, 137 (2002).

[30] J. W. Cahn, Phase separation by spinodal decomposition in isotropic systems, J. Chem. Phys. **42**, 93 (1965).
[31] V. Kendon, M. E. Cates, I. Pagonabarraga, J.-C. Desplat, and P. Bladon, Inertial effects in three-dimensional spinodal decomposition of a symmetric binary fluid mixture: A lattice Boltzmann study, J. Fluid Mech. **440**, 147 (2001).
[32] I. Pagonabarraga, J.-C. Desplat, A. J. Wagner, and M. E. Cates, Interfacial dynamics in 3D binary fluid demixing: Animation studies, New J. Phys. **3**, 9 (2001).
[33] R. Seemann, S. Herminghaus, and K. Jacobs, Dewetting Patterns and Molecular Forces: A Reconciliation, Phys. Rev. Lett. **86**, 5534 (2001).
[34] J. N. Israelachvili, *Intermolecular and Surface Forces*, 2nd ed. (Academic Press, London, 1991).
[35] P. Guenoun, R. Gastaud, F. Perrot, and D. Beysens, Spinodal decomposition patterns in an isodensity critical binary fluid: Direct-visualization and light-scattering analyses, Phys. Rev. A **36**, 4876 (1987).
[36] C. Sanborn, K. F. Ludwig, M. C. Rogers, and M. Sutton, Direct Measurement of Microstructural Avalanches During the Martensitic Transition of Cobalt Using Coherent X-Ray Scattering, Phys. Rev. Lett. **107**, 015702 (2011).
[37] G. Brown, P. A. Rikvold, M. Sutton, and M. Grant, Speckle from phase-ordering systems, Phys. Rev. E **56**, 6601 (1997).
[38] G. Brown, P. A. Rikvold, M. Sutton, and M. Grant, Evolution of speckle during spinodal decomposition, Phys. Rev. E **60**, 5151 (1999).
[39] A. Fluerasu, M. Sutton, and E. M. Dufresne, X-Ray Intensity Fluctuation Spectroscopy Studies on Phase-Ordering Systems, Phys. Rev. Lett. **94**, 055501 (2005).
[40] M. W. Kim, A. J. Schwartz, and W. I. Goldburg, Evidence for the Influence of Hydrodynamics in a Phase-Separating Fluid, Phys. Rev. Lett. **41**, 657 (1978).
[41] E. D. Siggia, Late stages of spinodal decomposition in binary mixtures, Phys. Rev. A **20**, 595 (1979).
[42] H. Furukawa, Effect of inertia on droplet growth in a fluid, Phys. Rev. A **31**, 1103 (1985).
[43] A. J. Wagner and J. M. Yeomans, Breakdown of Scale Invariance in the Coarsening of Phase-Separating Binary Fluids, Phys. Rev. Lett. **80**, 1429 (1998).
[44] V. S. Nikolayev, D. Beysens, and P. Guenoun, New Hydrodynamic Mechanism for Drop Coarsening, Phys. Rev. Lett. **76**, 3144 (1996).
[45] R. Shimizu and H. Tanaka, A novel coarsening mechanism of droplets in immiscible fluid mixtures, Nat. Commun. **6**, 7407 (2015).
[46] H. Tanaka, Viscoelastic phase separation, J. Phys.: Condens. Matter **12**, R207 (2000).
[47] R. Kirste and G. Porod, Röntgenkleinwinkelstreuung an kolloiden Systemen. Asymptotisches Verhalten der Streukurven, Kolloid Z. **184**, 1 (1962).
[48] C. Billotet and K. Binder, Dynamic correlation of fluctuations during spinodal decomposition, Physica A **103**, 99 (1980).